SEASONAL AND INTRA-SEASONAL VARIABILITY OF OCEAN THERMAL POTENTIAL ENERGY IN THE INDONESIAN EXCLUSIVE ECONOMIC ZONE

VARIABILITAS MUSIMAN DAN INTRA-MUSIMAN DARI ENERGI POTENSIAL PANAS LAUT DI ZONA EKONOMI EKSLUSIF INDONESIA

Totok Suprijo[1,2*], Gandhi Napitupulu[2], Nining Sari Ningsih[2], Denny Basardo Jonatan Sinaga[1], Audi Rachman[1]

[1] Coastal Oceanography Laboratory, Faculty of Earth Sciences and Technology, Bandung Institute of Technology, Bandung, Indonesia
[2] Research Group of Oceanography, Faculty of Earth Sciences and Technology, Bandung Institute of Technology, Bandung, Indonesia

*Corresponding author: totok.suprijo@itb.ac.id

(Received 20 January 2024; in revised from 30 January 2024; accepted 22 May 2024)

DOI : 10.32693/bomg.39.1.2024.866

ABSTRACT: Ocean thermal energy is a promising marine renewable energy resource that can be developed as a clean energy alternative for Indonesia, which is in the equatorial or tropical region. This study assesses the potential of ocean thermal energy as a renewable energy source in the Indonesian Exclusive Economic Zone (EEZ) by estimating the monthly, seasonal, and intra-seasonal variability of ocean thermal energy conversion (OTEC) resources. The Indonesian EEZ spans from 6°N to 11°S and 95°E to 139°E, covering an area of 3,495,698.72 km². Using temperature data from simulations of the Hybrid Coordinate Ocean Model (HYCOM), the study evaluates the potential of OTEC resources over a 50-year period (from January 1964 to December 2013) with a spatial resolution of 0.125°. Estimation of OTEC potential power resources was based on temperature differences at depths of 20 m and 1000 m, following the hybrid cycle working principle.The results of the estimations indicate that the area has a monthly average potential power of 289.73 GW. The estimation also reveals seasonal and intra-seasonal variability in this potential energy, with fluctuations ranging from 280.09 GW in August to 295.65 GW in December, influenced by phenomena such as ENSO (El Niño Southern Oscillation) and IOD (Indian Ocean Dipole). In the Indonesian EEZ, the average potential thermal power decreases to 288.23 GW during an El Niño event and increases to 291.72 GW during a La Niña event. The IOD phenomenon has a similar effect, with potential decreasing to 281.82 GW during a positive IOD event and rising to 292.64 GW during a negative IOD event.

Keywords: Indonesian Exclusive Economic Zone (EEZ), intra-seasonal variability, seasonal variability, ocean thermal energy conversion (OTEC)

ABSTRAK: *Energi panas laut adalah sumber daya energi terbarukan yang menjanjikan dan dapat dikembangkan sebagai alternatif energi bersih bagi Indonesia, yang berada di daerah khatulistiwa atau tropis. Kajian ini mengevaluasi potensi energi panas laut sebagai sumber energi terbarukan di Zona Ekonomi Eksklusif (ZEE) Indonesia dengan memperhitungkan variabilitas bulanan, musiman, dan intra-musiman dari konversi sumber daya energi panas laut (OTEC). ZEE Indonesia meliputi wilayah dari 6°Lintang Utara hingga 11°Lintang Selatan dan dari 95°Bujur Timur hingga 139°Bujur Timur, dengan luas mencapai 3.495.698,72 km². Dengan menggunakan data suhu dari simulasi Model Oseanografi Koordinat Hibrida (HYCOM), kajian ini mengevaluasi potensi sumber daya OTEC selama periode 50 tahun (Januari 1964 hingga*

Desember 2013) dengan resolusi spasial 0,125°. Estimasi sumber daya potensial energi OTEC didasarkan pada perbedaan suhu di kedalaman 20 m dan 1000 m, mengikuti prinsip kerja siklus hibrida. Hasil estimasi menunjukkan bahwa wilayah ZEE-Indonesia memiliki potensi daya rata-rata bulanan sebesar 289,73 GW. Hasil estimasi juga mengungkapkan adanya variabilitas musiman dan intra-musiman dari sumberdaya energi panas laut yang berfluktuasi dengan berkisaran dari 280,09 GW pada bulan Agustus dan 295,65 GW pada bulan Desember, serta dipengaruhi oleh fenomena seperti ENSO (El Niño Southern Oscillation) dan IOD (Indian Ocean Dipole). Di ZEE Indonesia, potensi rata-rata sumber daya panas laut mengalami penurunan menjadi 288,23 GW saat terjadi El Niño dan meningkat menjadi 291,72 GW pada peristiwa La Niña. Fenomena IOD memiliki efek serupa, potensi sumberdaya menurun menjadi 281,82 GW saat peristiwa IOD positif dan meningkat menjadi 292,64 GW ketika IOD negatif.

Kata Kunci: *Zona Ekonomi Eksklusif (ZEE) Indonesia, variabilitas intra-musiman, variabilitas musiman, konversi energi termal lautan (OTEC)*

INTRODUCTION

Ocean energy offers long-term carbon emission reduction potential. However, it is unlikely to make a significant contribution in the short term before 2020, as it is still in a nascent stage of development. All ocean energy technologies, except for tidal dams, are still conceptual, undergoing research and development, or are in the prototype and pre-commercial demonstration stages (Von Jouanne & Brekken, 2017). The performance of ocean energy technologies is expected to gradually improve as experience is gained and new technologies can access low-quality resources (Chu et al., 2020). Whether these technical advances will result in sufficient cost reductions to enable widespread deployment of ocean energy is a critical uncertainty in assessing the future role of ocean energy in climate change mitigation (Topper et al., 2019). While technical potential is not expected to be a major global barrier to ocean energy deployment, resource characteristics will require that local communities in the future choose among several available ocean technologies to suit local resource conditions (Rudolph et al., 2020).

Indonesia also has abundant resources for solar, wind, and ocean energy development. The country is located along the equator and covers a total tropical ocean area of approximately 7.9 million square kilometers, including the exclusive economic zone (Lubchenco & Haugan, 2023). Tropical seas naturally collect solar energy and absorb billions of watts of energy from the sun in the form of solar radiation every day (Merchant et al., 2019). Intense solar illumination and longer days result in significant warming of the upper 10 to 150 m of the ocean, resulting in warm ocean surface waters (27-29 °C) (Serban et al., 2021). This temperature difference represents a significant amount of potential energy, which would be a completely renewable energy source (Clemente et al., 2021). In addition to power generation using a method known as ocean thermal energy conversion (OTEC), this potential energy could be extracted to support heating, cooling, and transportation applications (Aresti et al., 2023).

For an OTEC factory to be economical, a temperature difference of about 20 °C is required. A temperature difference of this magnitude is available between surface water and water at a depth of 1000 m at most locations within 20° of the equators (Herrera et al., 2021; Langer et al., 2020). The electrical resources that can be extracted using OTEC plants from the world's oceans were estimated by a simple time-domain model of the one-dimensional ocean thermal structure (Bernal et al., 2022; Nihous, 2007). The published steady-state results were further extended by dividing the potential OTEC production region into one-degree "squares" and by allowing operational adjustment of OTEC operations. In that study, the 'OTEC production region' was based on the annual average temperature difference between 20 and 1000 m of water depth (Nihous, 2007). The study increased the estimated steady-state maximum OTEC electrical power from about 3 TW to 5 TW (Nihous, 2018). Recent results from the study, which assessed the OTEC rate with a high-resolution (0.125°×0.1251°) ocean general circulation model, indicated a global OTEC net maximum of about 12-14 TW (Rajagopalan & Nihous, 2013). Based on the vertical temperature difference criterion, a synthesis of relevant information to assess the feasibility of OTEC development in Indonesian waters was initiated (Bhuiyan et al., 2022). Utilizing temperature vertical profiles, a similar study to identify potential sites for OTEC development in Indonesian waters was conducted (Nihous, 2018). Although both previous studies have described potential locations

for OTEC development, they did not estimate the number of electrical resources in the Indonesian waters.

This research aims to analyze the potential of ocean heat energy contained in the EEZ of Indonesian waters. Furthermore, knowing the seasonal and intra-seasonal variability of the potential for ocean thermal energy in the Indonesian EEZ based on simulation data from 1964 to 2013. The influence of intra-seasonal variability consists of the El Nino Southern Oscillation (ENSO) and the Indian Ocean Dipole (IOD).

METHODS AND MATERIALS

Data

The study area of this research is the Indonesian waters, with coordinates of 6°N - 11°S and 95°E - 139°E (Figure 1a). The data used in this study are temperature data from the 3-dimensional hydrodynamic model Hybrid Coordinate Ocean Model (HYCOM). This data comes from research conducted by Rachmayani et al. (2023). The temperature data used is the monthly temperature at two depths, namely 20 m and 1000 m, in the period of January 1964 to December 2013 (50 years). This data has a spatial resolution of 0.125°×0.125°, resulting in a grid size of 353 × 137.

Sea surface temperature data (20 m) from buoy measurements were used to validate the surface temperature data (20 m) from the model. Buoy data were obtained from the Triangle Trans-Ocean Buoy Network (TRITON) measurement station in the Pacific Ocean and the Research Moored Array for African-Asian-Australian Monsoon Analysis and Prediction (RAMA) in the Indian Ocean, obtained from the National Oceanic and Atmospheric Administration (NOAA). Details of the validation of field data and model data are shown in Table 1, with the location of the stations shown in Figure 1a. Validation of model data with observation data has a bias value of 0.09 to 0.62 °C, indicating that the model temperature data is quite close to the field measurement data.

The average ocean temperatures at 20 m (Figure 1b) and 1000 m (Figure 1c) depths during 1964-2013 were 29.30 °C and 4.3 °C, respectively. The amount of variation in the temperature of Indonesian waters at a depth of 20 m can be shown through the standard deviation value. The standard deviation of Indonesian water temperature at a depth of 20 m ranges from 0.30 °C to 1.88 °C. The standard deviation of Indonesian water temperature at 1000 m depth ranges from 0.02 °C to 0.51 °C. This shows the

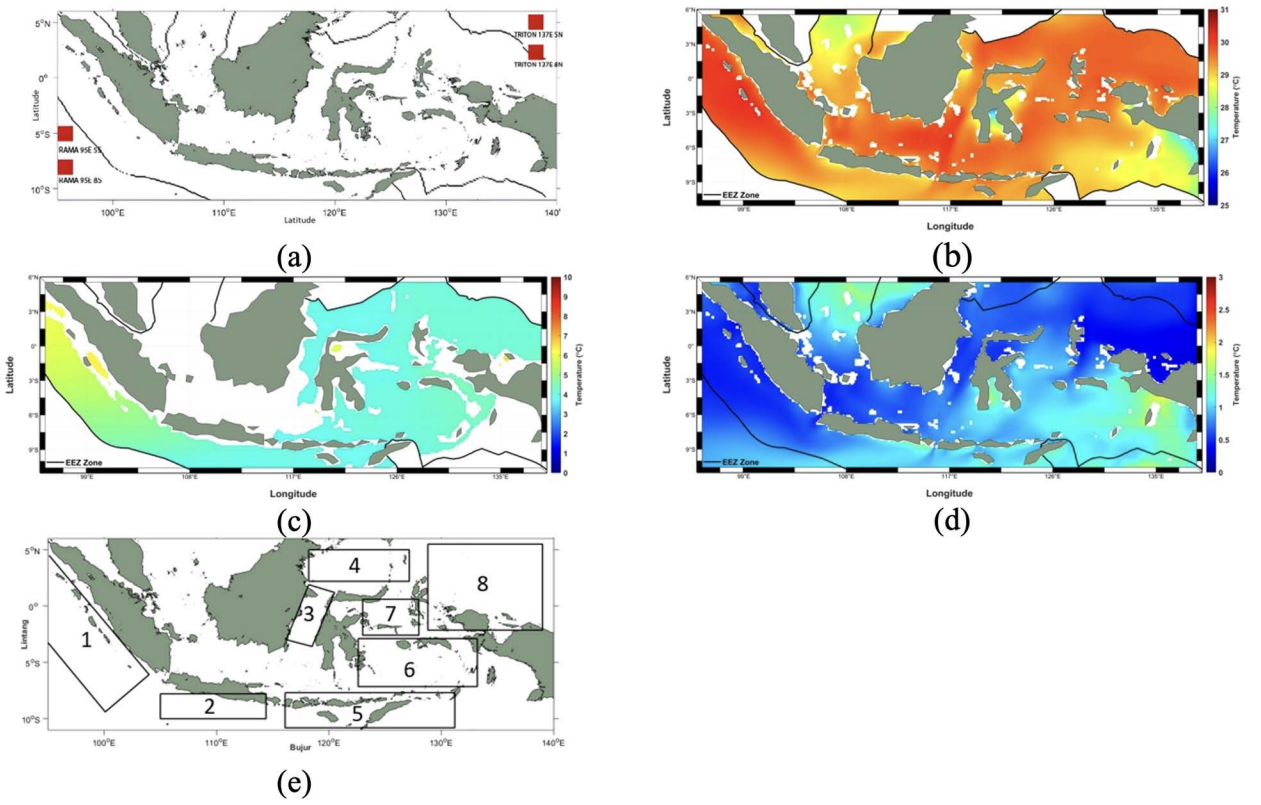

Figure 1. (a) Location points of measurement data of TRITON and RAMA stations. Average depth temperature of (b) 20 m and (c) 1000 m during 1964-2013. (d) The standard deviation of Indonesian water temperature at 20 m depth. (e) Division of the study area into eight observation areas.

stability of Indonesian water temperature at a depth of 1000 m. The small standard deviation indicates that the temperature in these waters tends to be stable.

In this study, the study area was divided into eight regions, as shown in Figure 1e, with details in Table 2. The division of the study area was conducted to determine how much influence the regional phenomenon has on each study area.

Data on the Oceanic Niño Index (ONI) and Dipole Mode Index (DMI) are utilized to examine variations in ocean temperature and power potential about the ENSO and IOD phenomena. ONI data was acquired from NOAA's Climate Prediction Center, while DMI data was obtained from NOAA's Physical Science Laboratory.

Table 1. Validation of model data with field measurement data.

Coordinate Point	Period	Bias (℃)	*RMSE* (℃)
2° N; 137° E	May 1992 – May 2013	0.44	0.42
5° N;137° E	May 1993 – August 2007	0.62	0.54
5° S; 95° E	November 2001 – October 2012	0.37	0.49
8° S; 95° E	November 2009 – December 2013	0.09	0.51

Table 2. Details of the division of the study area

Region	Longitude	Latitude
Region 1 (Indian Ocean)	95° E; 104° E	9.4° S; 4.5° N
Region 2 (South of Java)	105° E; 114.4° E	10° S; 7.8° S
Region 3 (Makassar Strait)	116.2° E; 120.5° E	3.6° S; 1.9° N
Region 4 (Sulawesi Sea)	118.2° E; 127.25° E	2.2° N; 5.5° N
Region 5 (Sawu Sea and Arafura Sea)	116.1° E; 131.2° E	10.8° S; 7.7° S
Region 6 (Banda Sea and Seram Sea)	122.6° E; 133.2° E	7.16° S; 2.9° S
Region 7 (Maluku Sea)	123° E; 128° E	2.6° S; 0.6° S
Region 8 (Pacific Ocean)	128.8° E; 139° E	2.5° S; 5.5° N

Method

OTEC is an old idea that solar energy is stored as heat in the mixed layer (surface) of tropical oceans (Nihous, 2005). The heat in the ocean can be utilized for electrical energy through OTEC. The working principle of OTEC is based on the thermodynamic cycle, the Rankine cycle, which can convert heat into work. Based on the way of working, OTEC can be divided into three types, namely Open Cycle, Closed Cycle, and Hybrid Cycle (Aresti et al., 2023).

The working principle of the Open Cycle is to use warm water at sea level to drive the turbine. A mass of warm water is pumped into a low-pressure container, causing the water to boil. The water vapor will drive the turbine to generate electricity. The vapor will be re-condensed using a mass of cold water from the depths (Herrera et al., 2021). The working principle of the Closed Cycle is to utilize the temperature difference between warm water and cold water used as working fluid (ammonia is generally used) to complete the Rankine cycle (Zhang et al., 2021). The warm water mass is used to vaporize the working fluid, and then the working fluid vapor will pass through the generator to generate electricity. The cold-water mass is used to make the working fluid liquid again so that it can be used to repeat the cycle. The working principle of the Hybrid Cycle is to use the advantages of the Open Cycle and Closed Cycle. A mass of warm seawater is put into a low-pressure container so that the water will boil. The water vapor is used to vaporize the low-pressure fluid that will drive the turbine to generate electricity (Wang et al., 2022). The water vapor will be re-condensed using a mass of cold water (Masutani & Takahashi, 2001).

OTEC power potential is obtained by calculating the temperature difference (ΔT) between 20 m and 1000 m depth using the working principle of the Hybrid Cycle (equation 1). Based on Nihous (2007), OTEC can be operated if ΔT has a value of more than 20 °C. The value of each parameter for the OTEC calculation is shown in Table 3.

$$P_{net} = \frac{Q_{cw}\rho c_p \epsilon_{tg}}{8T}\left\{\frac{3\gamma}{2(1+\gamma)}\Delta T^2 - 0.18\Delta T^2 - 0.12\left(\frac{\gamma}{2}\right)^{2.75}\Delta T^2\right\} \quad (1)$$

The total power potential is obtained by summing up all the power from each existing data grid with Equation 2.

$$\sum_{m=0}^{353}\sum_{n=0}^{137} P_{(m,n)} \quad (2)$$

where m is the grid longitude, n is the grid latitude, and P is the power potential value at the grid latitude and longitude.

Model data validation was performed to ensure that the data was fit for research. Validation is done

Table 3. Parameter values for OTEC calculation

Parameter	Value	Unit	Meaning of symbol
Q_{cw}	2.43	m^3/s	Cold water discharge
ρ	1025	kg/m^3	Density of seawater
$\overline{c_p}$	4000	J/kg°C	Specific heat of seawater
ε_{tg}	0.85	-	Turbogenerator efficiency
γ	2	-	Comparison of Q_{cw} with Q_{ww}
ΔT	$\Delta T(x,y)$	°C	Difference between T_{20} and T_{1000}
T	$T(x,y)$	°C	20 m depth temperature

by comparing model data with observation data through bias and *RMSE* calculations with the formulation by Thomson and Emery (2014) as follows:

$$bias = \frac{1}{n}\sum_{i=1}^{n}(T_m - T_0) \quad (3)$$

$$RMSE = \sqrt{\frac{1}{n}\sum_{i=1}^{n}(T_m - T_0)^2} \quad (4)$$

where T_m is the modeled temperature (°C), T_0 is the observed temperature (°C), n is the amount of data.

RESULTS AND DISCUSSION

Seasonal Variations in Indonesian Waters Temperatures

The average temperature value for each month can be seen in Table 4. The highest average temperature was in April at 29.72 °C and the lowest was in August at 28.61 °C. This is influenced by the apparent movement of the sun. In April, the sun is just above the equator moving north, so the average sea surface temperature is high. Meanwhile, in August, just above the equator, the sun is moving south, towards the equator. This causes the average value of surface temperature in Indonesian waters to be low.

The average ocean temperature at 20 m depth in Indonesian waters varies seasonally, as shown in Figure 2. The average ocean temperature at 20 m depth in the west monsoon season is 29.40 °C, in the first transition season 29.62 °C, in the east monsoon season 28.92 °C, and in the second transition season 29.26 °C.

In the west monsoon season (Figure 2a), the temperature of the waters in the northern part of Indonesia at a depth of 20 m is lower than in the southern part of Indonesia. This is due to the position of the sun south of the equator, so the temperature of the waters in southern Indonesia is higher. In the transitional season (Figure 2b), the average value of surface temperature is also high because the position of the sun is just above the equator. Whereas in the east monsoon season (Figure 2c), the position of the sun is north of the equator, so the temperature of the waters of northern Indonesia is higher. In addition, during the east monsoon season, there is cooling in the upwelling zone south of Java and the Arafura Sea, where the water mass moves to the Java Sea and the Karimata Strait, so to compensate for this, there is an increase in cold water mass from depth (Qu et al., 2015).

The average ocean temperature at 1000 m depth in the west monsoon season is 4.30 °C (Figure 2e), in the first transition season 4.34 °C (Figure 2f), in the east monsoon season 4.27 °C (Figure 2g), and in the second transition season 4.31 °C (Figure 2h). The temperature at a depth of 1000 m does not have a significant difference every season because the influence of the sun is not significant to the change in temperature at a depth of 1000 m. The variation of temperature at a depth of 1000 concerning season and year is <0.5 °C, so the depth of 1000 is used as a reference depth for calculating OTEC values.

Table 4. Average Temperature Values at 20 m Depth in the Indonesian Sea

Month	Temperature (°C)		Month	Temperature (°C)	
	20 m	1000 m		20 m	1000 m
January	29.31	4.29	July	28.83	4.29
February	29.25	4.32	August	28.61	4.32
March	29.47	4.35	September	28.82	4.35
April	29.72	4.35	October	29.31	4.35
May	29.68	4.33	November	29.65	4.33
June	29.30	4.29	December	29.65	4.29

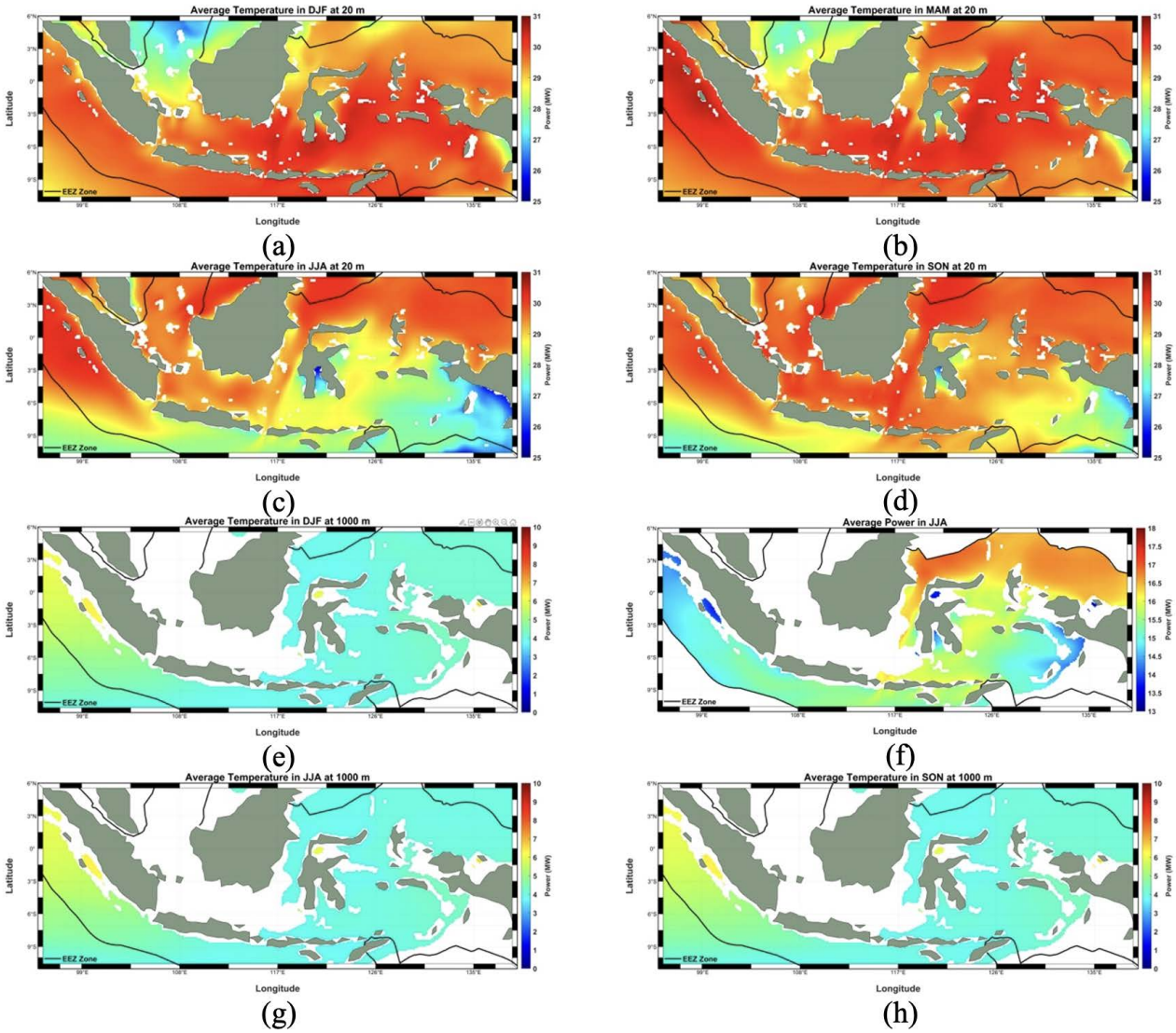

Figure 2. Average 20 m depth temperature in Seasons (a) West, (b) Transition 1, (c) East, and (d) Transition 2. Average 1000 m depth temperature in Seasons (e) West, (f) Transition 1, (g) East, and (h) Transition 2.

Influence of Intraseasonal Variations on Indonesian Sea Surface Temperature

The dominant intraseasonal phenomena that influence surface temperature in Indonesian waters, namely ENSO and IOD. The ENSO phenomenon in the Pacific Ocean and the IOD in the Indian Ocean affect variations in Indonesia's sea surface temperature. Based on historical records of the ENSO phenomenon, it is known that there were 17 times El Nino and 15 times La Nina in the period 1964-2013. Table 5 suggests a potential link between ENSO and Indonesian sea surface temperatures. While the temperature differences between El Niño (Figure 3b) and normal conditions (Figure 3a) appear minimal and La Niña (Figure 3c) conditions show a slight increase compared to normal, further analysis is required to determine the statistical significance of these variations. This is because when El Nino occurs, warm water masses in the Pacific Ocean move eastward or away from Indonesian waters so that the surface temperature of Indonesian waters decreases. Meanwhile, when La Nina occurs, warm water masses are pushed westward or enter Indonesian waters, so that the surface temperature of Indonesian waters increases.

Based on historical records of the IOD phenomenon, it is known that there were 7 times positive IOD and 7 times negative IOD in the period 1964-2013. When a positive IOD (Figure 3f) occurs, the surface temperature of Indonesian waters will be lower than when no IOD phenomenon occurs (Figure 3d). This is because when positive IOD (Figure 3f) occurs, the warm water mass in the Indian Ocean is in the western part of western African waters. Meanwhile, when a negative IOD occurs (Figure 3e), the warm water mass in the Indian Ocean is in the eastern or

western part of Indonesia. This causes the surface temperature of Indonesian waters to increase.

When the El Nino phenomenon occurs, it causes a decrease in average temperature at all peaks of the El Nino phenomenon except in October 1969 and July 1987. The largest decrease in average temperature occurred in October 1965, with an ONI of 2. The temperature decrease varied from -0.08 to -1.43 °C. The largest decrease in average temperature occurred in the Maluku Sea at -1.43 °C. The El Nino phenomenon also causes an increase in temperature in the Indian Ocean area and south of Java at certain times, which is due to an increase in average temperature in the Malacca Strait and Java Sea. The El-Nino phenomenon also caused an increase in average temperature in the Arafura Sea, Banda Sea, and Seram Sea in October 1969, November 1976, December 1979, and July 1987. The average temperature increase varied from 0.05 to 0.68 °C. The largest average temperature increase occurred in the Indian Ocean by 0.68 °C.

When the La-Nina phenomenon occurs, it causes an increase in average temperature at all peaks of the La-Nina phenomenon except in December 1984 and December 1995. The largest increase in average temperature occurred in January 1999, with an ONI of -1.7. The influence of the La-Nina phenomenon on changes in average temperature in western Indonesian waters such as the Indian Ocean and southern Java is not as strong as the El Nino phenomenon. This is shown by the increase and decrease in temperature caused by the La Nina phenomenon in the Indian Ocean and southern Java, which has the same amount at all peak events. The temperature increase that occurred varied in each study area by 0.06 to 0.92 °C. The largest temperature increase occurred in the Maluku Sea by 0.92 °C.

Table 5. Average Indonesian sea temperature at 20 m depth during IOD and ENSO phenomena

Condition	Average Temperature (°C)	Condition	Average Temperature (°C)
Absence of ENSO	29.29	Absence of IOD	29.33
El Nino	29.22	IOD (+)	28.81
La Nina	29.39	IOD (-)	29.31

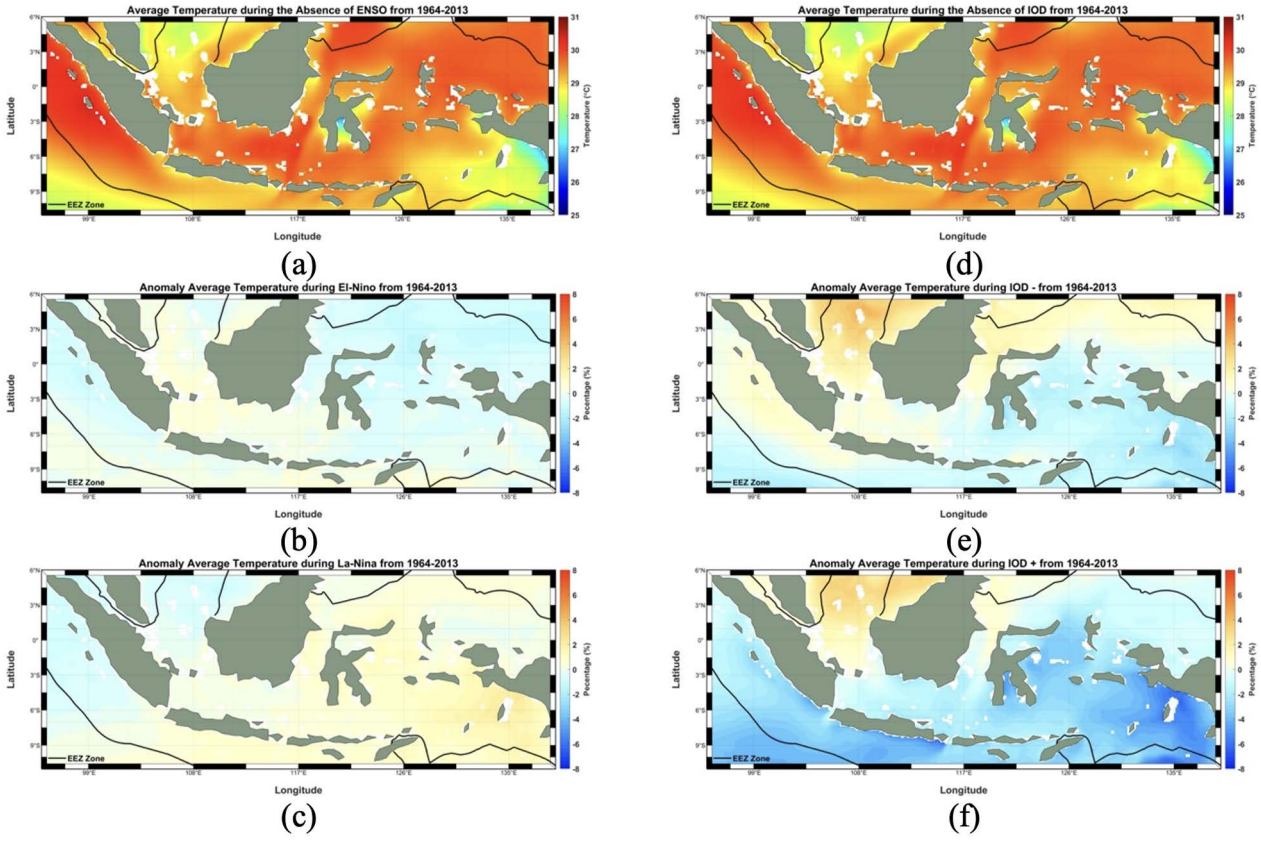

Figure 3. Average 20 m depth temperature during (a) absence of ENSO, (b) El Nino, (c) La Nina, (d) absence of IOD, (e) IOD (-), and (f) IOD (+) from 1964 to 2013.

In addition to the ENSO phenomenon that occurs in the Pacific Ocean, temperature variations in Indonesian waters are also influenced by the IOD phenomenon in the Indian Ocean. During the Positive IOD, the largest decrease in average temperature occurred in the southern region of Java by -1.40 °C. When the Negative IOD phenomenon occurs, it also causes a decrease in temperature, except in the Indian Ocean, Makassar Strait, and Sulawesi Sea. The largest average temperature decrease occurred in the Banda Sea and Seram Sea by -0.66 °C.

When the Positive IOD phenomenon occurs, it causes a decrease in average temperature at all peaks. The largest decrease in average temperature occurred in August 1994, with a DMI of 0.923. The temperature decrease varied from -0.24 to -1.03 °C in each study area. The largest temperature decrease occurred in southern Java at -1.03 °C. However, the Positive IOD phenomenon also caused an increase in average temperature in the Indian Ocean area in July 1983, in the Makassar Strait area in October 2012, in the Sulawesi Sea area in October 2012, and in the Pacific Ocean area in October 2012. The largest temperature increase occurred in the Makassar Strait area by 0.41 °C.

When the Negative IOD phenomenon occurs, it causes an increase in average temperature at all peaks except in September 1992. The largest average temperature increase occurred in October 1996, with a DMI of -0.949. The average temperature increase varied from 0.07 to 0.46 °C. The largest temperature increase occurred in southern Java by 0.46 °C. The Negative IOD phenomenon in September 1992 caused a decrease in average temperature in all study areas except the Indian Ocean and southern Java. The largest decrease in average temperature occurred in the Maluku Sea area by -0.32 °C.

Seasonal Influence on OTEC Potential in EEZ Indonesia

The OTEC power potential is calculated based on the temperature difference between warm surface water (typically at a depth of 20 m) and deep, cold water (usually around 1000 m). While Masutani and Takahashi (2001) suggest a minimum temperature difference of 20°C for OTEC operation, this significant temperature differential is only found in deep sea areas of the Indonesian waters. Indonesia's EEZ area of 3,485,698.72 km² stores potential OTEC resources as shown in Figure 4. The ΔT value in Indonesian waters varies between 22.84°C and 26.77°C. The variation of ΔT is dominantly influenced by the variation of 20 m depth temperature because the variation of 1000 m depth temperature is almost nonexistent.

Indonesia's potential for OTEC varies across regions, with the northern and eastern parts generally favored due to cooler deep waters and a larger temperature gradient compared to the western regions. This gradient, driven by the average temperature difference at a depth of 1000 m, is crucial for OTEC power generation. Based on average power density potential, the regions with the highest OTEC potential are Region 4 (Sulawesi Sea), Region 6 (Banda Sea and Seram Sea), Region 2 (South Java), Region 7 (Maluku Sea), Region 8 (Pacific Ocean), Region 1 (Indian Ocean), Region 5 (Sawu Sea and Arafura Sea), and Region 3 (Makassar Strait). While Figure 4 suggests a higher average total power for Region 1, further investigation into factors beyond temperature difference, such as water flow patterns and current speeds, is needed for a more comprehensive assessment.

The monthly power potential experiences variations due to the monthly ΔT variations. The highest average monthly power potential is in December, reaching 295.65 GW, as shown in Figure 4a. In December, the sun is positioned south of the equator, causing the surface temperature in southern Indonesia to increase. This leads to an increase in the average ΔT and the overall potential for average power. Meanwhile, the lowest average monthly power potential is in August, at 280.09 GW (Figure 4b). This is because the sun, during August, moves northward towards the equator in Indonesia, resulting in a decrease in the overall surface temperature and average ΔT of Indonesian waters.

Seasonal variation is also observed in the ocean's thermal energy potential. The highest average seasonal power potential is during the transitional season I (MAM), at 293.91 GW, as depicted in Figure 4d. Meanwhile, the lowest average seasonal power potential is during the east monsoon season (JJA), shown in Figure 4e, at 284.18 GW. This corresponds to the seasonal variation in the temperature at a depth of 20 m. During the transitional season I, the sun is directly above Indonesia, causing an increase in sea surface temperature and, consequently, an increase in power potential. In contrast, during the east monsoon season, the sun is north of the equator, leading to a decrease in the sea surface temperature in Indonesia and a reduction in the average power potential.

The average power density in each study area is illustrated in Figure 4e. The order of regions with the

highest to lowest average power density potential is Region 4 (Sulawesi Sea), Region 6 (Banda Sea and Seram Sea), Region 2 (South Java), Region 7 (Maluku Sea), Region 8 (Pacific Ocean), Region 1 (Indian Ocean), Region 5 (Sawu Sea and Arafura Sea), and Region 3 (Makassar Strait).

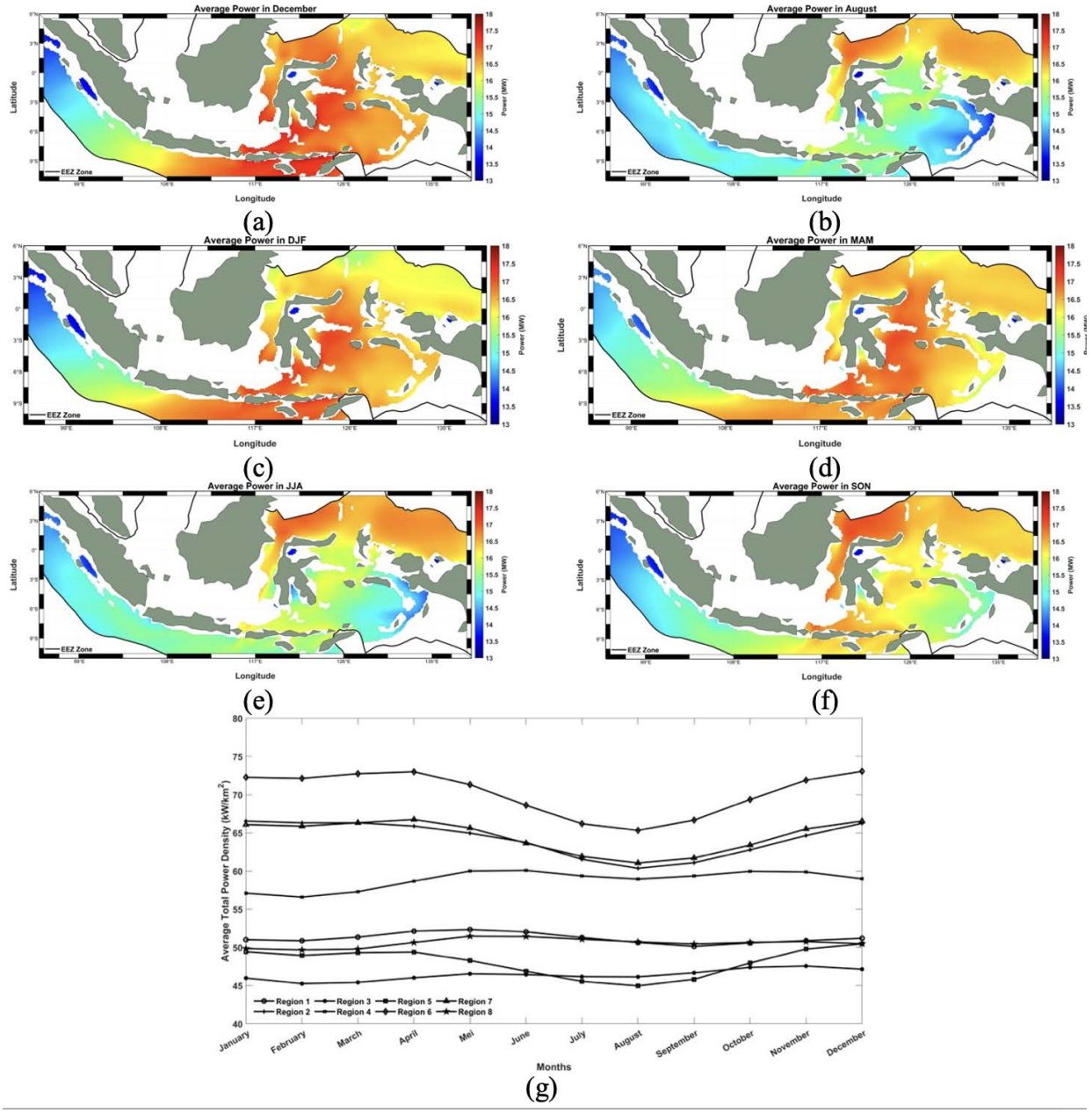

Figure 4. Average power potential of Indonesian Ocean thermal energy in the months of (a) December and (b) August and the seasons of (c) DJF, (d) MAM, (e) JJA, and (f) SON during 1964-2013. (g) The average power density potential of the Indonesian Ocean thermal energy each month in each division of the study area.

The Influence of ENSO and IOD on OTEC Potential in EEZ Indonesia

Changes in ocean temperature variations directly impact the potential for OTEC in Indonesia, as shown in Table 6. OTEC relies on a significant temperature difference between warm surface waters and deep, cold waters. During El Niño events (Figure 5b), when sea surface temperatures generally decrease slightly (as discussed earlier), the temperature difference between surface and deep water also shrinks. This reduction in the temperature gradient leads to a decrease in the total OTEC power potential compared to normal conditions (Figure 5a). Conversely, La Niña events (Figure 5c) are often associated with slightly warmer surface waters, which can increase the temperature difference with

deep water, thus enhancing the overall OTEC potential in Indonesian waters.

The reduction in power potential in each study area varies from -0.07% to -6.48%. The El Niño phenomenon (Figure 5b) causes a more significant decrease in power in the eastern waters of Indonesia, such as in the Sawu Sea and Arafura Sea, Banda Sea and Seram Sea, and Maluku Sea, compared to other regions. The power potential decrease in the Sawu Sea and Arafura Sea reaches -5.40%, followed by -5.64% in the Banda Sea and Seram Sea, and -6.48% in the Maluku Sea. In addition to the reduction in power potential, the El Niño phenomenon also led to an increase in power potential in the Indian Ocean region in December 1979 and July 1987, in South Java in January 1969, December 1979, July 1987, January 1992, December 1994, and December 2009, in the Makassar Strait in January 1992, December 1994, November 2002, and December 2009, in the Sulawesi Sea in November 2002, Sawu Sea and Arafura Sea in December 1979, July 1987, January 1992, December 1994, November 2002, and December 2009, in the Banda Sea and Seram Sea in December 1979, July 1987, December 1994, and December 2009, in the Maluku Sea in October 1969, November 1976, November 1977, December 1979, and December 1994, and the Pacific Ocean in November 2002. The Indian Ocean region in July 1987 experienced the largest increase in power potential compared to other regions, reaching 3.35%.

When a weak El Niño event occurs (ONI: 0.5-0.9) during the west monsoon season, the power decrease is not significant (less than 1%) across all study areas. This is because the seasonal influence is still strong, as seen by the additional power in the southern regions such as the Indian Ocean, Arafura Sea, and Seram Sea. However, during a moderate El Niño event (ONI: 1.0-1.4) in the west monsoon season, a significant power decrease is observed in the Indian Ocean, Banda Sea, Seram Sea, Maluku Sea, and the Pacific Ocean. In the case of a strong El Niño event (ONI: ≥1.5) during the west monsoon

Table 6. Impact of ENSO and IOD Phenomena on Total Power Potential

Condition	Power potential total (GW)	Condition	Power potential total (GW)
Normal	290.28	Normal	290.28
El-Nino	288.23	IOD (+)	281.92
La-Nina	291.72	IOD (-)	292.64

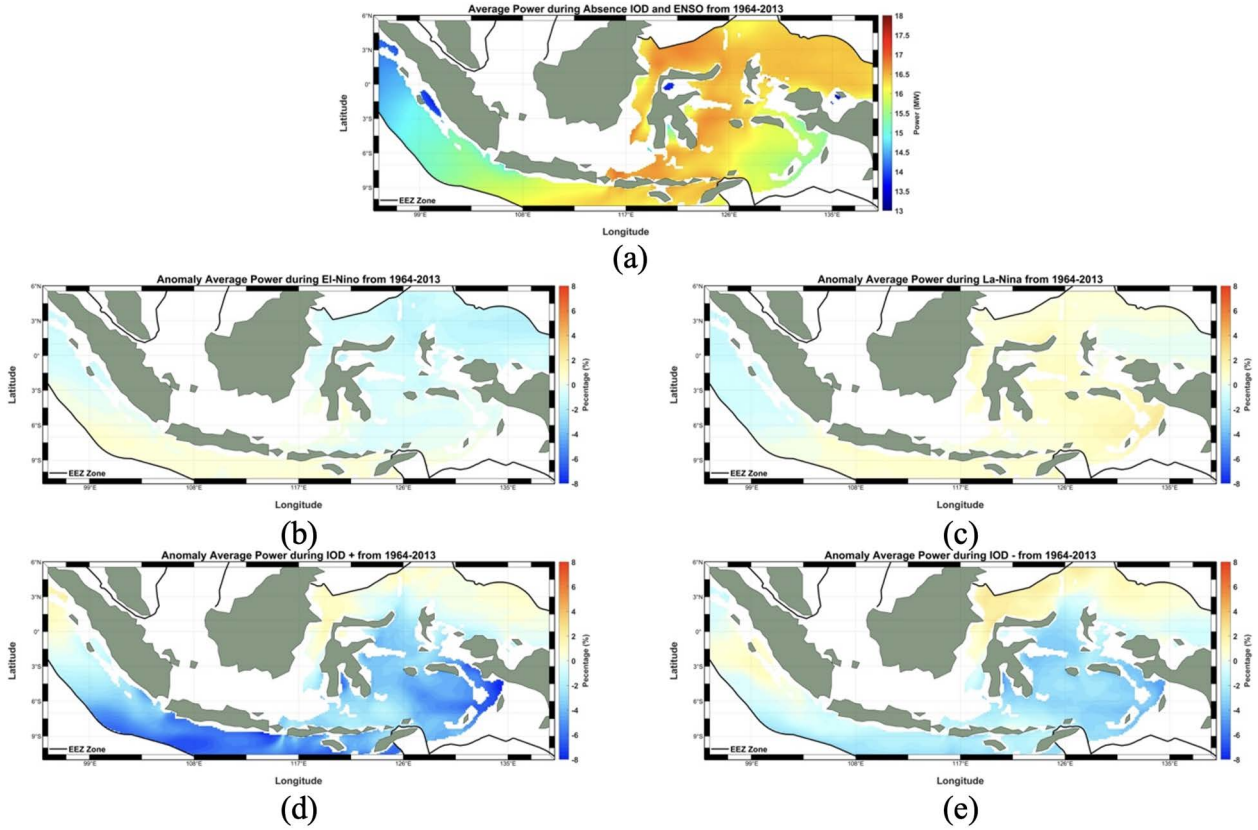

Figure 5. Anomaly of power potential in the study areas during (a) absence of ENSO and IOD, (b) El-Nino, (c) La-Nina, (d) IOD (+), and (e) IOD (-) phenomena.

season, a more substantial power decrease (over 2.5%) occurs in the Makassar Strait, Sulawesi Sea, Sawu Sea and Arafura Sea, Banda Sea and Seram Sea, and Maluku Sea.

The La Niña phenomenon has a minimum impact on power changes in the Indian Ocean (Figure 5c). La Niña causes variable increases in power potential in each study area, ranging from 0.14% to 4.91%. The influence of La Niña on power potential changes is not as significant as that of El Niño, but it leads to substantial increases in potential power in all study areas except the Indian Ocean and the Pacific Ocean. La Niña results in a power increase of 4.72% in South Java, 3.80% in the Makassar Strait, 4.76% in the Sulawesi Sea, 4.80% in the Sawu Sea, and Arafura Sea, 4.91% in the Banda Sea and Seram Sea, and 4.08% in the Maluku Sea.

Similar to El Niño, La Niña does not always cause an increase in power potential in each study area. In fact, during La Niña in December 1970, there was a decrease in power potential across all study areas. The power potential decrease varied from -0.21% to -3.78% in each study area, with the largest decrease occurring in the Pacific Ocean in December 1970 at -3.78%.

OTEC, a technology that utilizes the temperature difference between warm surface and deep, cold ocean waters, presents exciting potential for Indonesia as a renewable energy source. However, its viability is intricately linked to the complex interplay of climate patterns, particularly the ENSO and the IOD. ENSO, with its warm (El Niño) and cool (La Niña) phases, significantly influences OTEC potential through overall sea surface temperature variations. El Niño events, characterized by slightly cooler surface waters, diminish the temperature gradient between surface and deep waters, reducing OTEC potential. Conversely, La Niña events, with their tendency for slightly warmer surface waters, amplify the temperature gradient, enhancing OTEC potential. IOD, another key climate influence, further modulates OTEC potential through the spatial distribution of sea surface temperatures. Positive IOD events, marked by warmer waters in the western Indian Ocean and cooler waters in the east, tend to decrease the temperature gradient in Indonesia, leading to lower OTEC potential (as shown in Table 6). In contrast, Negative IOD events, with cooler western and warmer eastern waters, enhance the temperature gradient, particularly in the eastern Indian Ocean region, increasing OTEC potential (as detailed in Table 7).

Positive Indian Ocean Dipole (IOD) events (Figure 5d) induce varying reductions in OTEC power potential across Indonesia, ranging from -0.10% to -4.44% in different study areas. While the text describes a substantial decrease in the Indian Ocean (-3.92%), Table 7 reveals a smaller decrease for Region 1 within this region (-1.56%). This highlights the importance of spatial variability within regions during Positive IOD events. Further investigation into the specific timeframes and averaging methods used for regional data in Table 7 is recommended for a more nuanced understanding.

Table 7 presents estimations of how ENSO and IOD phenomena influence average power potential changes in each study area. Positive IOD events generally cause larger variations in power potential compared to other phenomena. Based on this table, the South Java region emerges as a potential candidate for OTEC development due to its relatively stable response to both ENSO and IOD events (as evidenced by a smaller range of power changes). Conversely, the Sawu Sea, Arafura Sea, and Maluku Sea exhibit a wider range of power changes due to ENSO and IOD influences, making them less favorable locations for OTEC development.

Negative IOD events (Figure 5e) generally lead to increases in total power potential, with exceptions like September 1992. However, Table 7 also suggests potential decreases in specific regions and months during Negative IOD events. This underscores the complexity of IOD's impact and the need for further

Table 7. Power Potential in Study Areas during ENSO and IOD Phenomena.

Region	Power potential total (GW) (Normal)	Increasing/Decreasing Power Potential (%)			
		El-Nino	La-Nina	IOD (+)	IOD (-)
Region 1	42.95	-0.21	-0.69	-1.56	-0.06
Region 2	17.96	0.77	1.05	-5.71	-1.27
Region 3	7.62	-0.43	0.89	0.54	1.04
Region 4	19.66	-0.98	0.58	0.20	1.35
Region 5	28.39	0.28	0.74	-4.14	-2.03
Region 6	40.98	-0.35	1.07	-4.17	-2.95
Region 7	8.73	-0.74	1.01	-3.33	-3.18
Region 8	52.99	-1.16	0.13	-0.14	0.12

analysis to fully comprehend its influence on OTEC potential. Disentangling the individual contributions of IOD and ENSO, particularly when they co-occur, remains a challenge. Future research endeavors could explore statistical methods to isolate these climate patterns' effects on OTEC potential variations in Indonesia.

CONCLUSSIONS

We obtained that temperature data validation between the model and the observation shows a good agreement with a bias ranging from -0.43°C to 0.09°C and a Root Mean Square Error (RMSE) ranging from 0.42°C to 0.54°C. The monthly average temperature in Indonesian EEZ at a depth of 20 m varies between 24.35°C (in August) and 31.24°C (in December), with a standard deviation of 0.83°C. At a depth of 1000 m, which is used as the reference depth, the average monthly water temperature in Indonesian waters ranges from 2.84°C to 7.88°C, with a standard deviation of 0.09°C that indicates stable temperature with small variability. The average estimation of potential thermal power energy in the Indonesian EEZ, represented by 3,495,698.72 km², is 289.73 GW. This potential power varies in monthly average with a minimum value of 280.09 GW occurring in August and reaching a maximum value of 295.65 GW in December. In 50 years span from 1964 to 2013, we found that the highest seasonal average potential power of ocean thermal energy in Indonesian EEZ is 293.91 GW which occurs during transition season I (March, April, and May). On the other hand, the lowest value, i.e. 284.18 GW, of seasonal average potential power occurs in the east monsoon season (December, January, and February). Furthermore, intra-seasonal variability potential thermal power energy in Indonesian EEZ occurs due to ENSO and IOD. During El-Nino events, the potential power energy decreases to 288.23 GW on a monthly average, whereas at La-Nina events, it increases to 291.72 GW also on a monthly average. In addition, the monthly average of potential thermal power in the same zone decreases to 281.82 GW when positive IOD occurs, and on the contrary, it increases on average to 292.64 GW during negative IOD events. The order of regions with the highest to lowest average power density potential, which are considered potential locations for OTEC development, is as follows: Region 4 (Sulawesi Sea), Region 6 (Banda Sea and Seram Sea), Region 2 (South Java), Region 7 (Maluku Sea), Region 8 (Pacific Ocean), Region 1 (Indian Ocean), Region 5 (Sawu Sea and Arafura Sea), and Region 3 (Makassar Strait).

REFERENCES

Aresti, L., Christodoulides, P., Michailides, C., & Onoufriou, T., 2023. Reviewing the energy, environment, and economy prospects of Ocean Thermal Energy Conversion (OTEC) systems. *Sustainable Energy Technologies and Assessments*, 60, 103459. https://doi.org/10.1016/J.SETA.2023.103459

Bernal, E. M., Garrido, D. C., Perea, G. A., & Escobedo Trujillo, B. A., 2022. Assessment of potential and temperature differential for an ocean thermal energy conversion plant. Case study: Cozumel, Mexico. *2022 IEEE International Conference on Engineering Veracruz, ICEV 2022*. https://doi.org/10.1109/ICEV56253.2022.9959202

Bhuiyan, M. A., Hu, P., Khare, V., Hamaguchi, Y., Thakur, B. K., & Rahman, M. K., 2022. Economic feasibility of marine renewable energy: Review. *Frontiers in Marine Science*, 9, 988513. https://doi.org/10.3389/FMARS.2022.988513/BIBTEX

Chu, W., Calise, F., Duić, N., Østergaard, P. A., Vicidomini, M., & Wang, Q., 2020. Recent Advances in Technology, Strategy and Application of Sustainable Energy Systems. *Energies 2020,* 13(19): 5229. https://doi.org/10.3390/EN13195229

Clemente, D., Rosa-Santos, P., & Taveira-Pinto, F., 2021. On the potential synergies and applications of wave energy converters: A review. *Renewable and Sustainable Energy Reviews*, 135, 110162. https://doi.org/10.1016/J.RSER.2020.110162

Herrera, J., Sierra, S., & Ibeas, A., 2021. Ocean Thermal Energy Conversion and Other Uses of Deep Sea Water: A Review. *Journal of Marine Science and Engineering 2021,* 9(4): 356. https://doi.org/10.3390/ JMSE9040356

Langer, J., Quist, J., & Blok, K., 2020. Recent progress in the economics of ocean thermal energy conversion: Critical review and research agenda. *Renewable and Sustainable Energy Reviews*, 130, 109960. https://doi.org/10.1016/J.RSER.2020.109960

Lubchenco, J., & Haugan, P. M., 2023. Coastal Development: Resilience, Restoration and Infrastructure Requirements. *The Blue Compendium*, 213-277. https://doi.org/ 10.1007/978-3-031-16277-0-7

Masutani, S. M., & Takahashi, P. K., 2001. Ocean Thermal Energy Conversion (otec). *Encyclopedia of Ocean Sciences*, 1993-1999. https://doi.org/10.1006/RWOS.2001.0031

Merchant, C. J., Minnett, P. J., Beggs, H., Corlett, G. K., Gentemann, C., Harris, A. R., Hoyer, J., & Maturi, E., 2019. Global Sea Surface Temperature. *Taking the Temperature of the Earth: Steps towards Integrated Understanding of Variability and Change*, 5-55. https://doi.org/10.1016/B978-0-12-814458-9.00002-2

Nihous, G. C., 2005. An Order-of-Magnitude Estimate of Ocean Thermal Energy Conversion Resources. *Journal of Energy Resources Technology*, 127(4): 328-333. https://doi.org/10.1115/1.1949624

Nihous, G. C., 2007. A Preliminary Assessment of Ocean Thermal Energy Conversion Resources. *Journal of Energy Resources Technology*, 129(1): 10-17. https://doi.org/ 10.1115/1.2424965

Nihous, G., 2018. A Preliminary Investigation of the Effect of Ocean Thermal Energy Conversion (OTEC) Effluent Discharge Options on Global OTEC Resources. *Journal of Marine Science and Engineering 2018,* 6(1): 25. https://doi.org/10.3390/ JMSE6010025

Qu, B., Song, J., Yuan, H., Li, X., Li, N., Duan, L., ... & Lu, X., 2015. Summer carbonate chemistry dynamics in the Southern Yellow Sea and the East China Sea: Regional variations and controls. *Continental Shelf Research*, 111, 250-261.

Rachmayani, R., Ningsih, N. S., Hanifah, F., & Nabilla, Y., 2023. Long-Term Trend and Variability of Volume Transport and Advective Heat Flux through the Boundaries of the Java Sea Based on a Global Ocean Circulation Model (1950–2013). *Water 2023,* 15(4): 740. https://doi.org/ 10.3390/ W15040740

Rajagopalan, K., & Nihous, G. C., 2013. An Assessment of Global Ocean Thermal Energy Conversion Resources With a High-Resolution Ocean General Circulation Model. *Journal of Energy Resources Technology*, 135(4). https://doi.org/10.1115/1.4023868

Rudolph, T. B., Ruckelshaus, M., Swilling, M., Allison, E. H., Österblom, H., Gelcich, S., & Mbatha, P., 2020. A transition to sustainable ocean governance. *Nature Communications 2020*, 11(1): 1-14. https://doi.org/ 10.1038/ s41467-020-17410-2

Serban, M., Li, G. yu, Serban, R. D., Wang, F., Fedorov, A., Vera, S., Cao, Y. peng, Chen, P. chao, & Wang, W., 2021. Characteristics of the active-layer under the China-Russia Crude Oil pipeline. *Journal of Mountain Science*, 18(2): 323-337. https://doi.org/ 10.1007/S11629-020-6240-Y/METRICS

Thomson, R. E., & Emery, W. J., 2014. Data analysis methods in physical oceanography. Newnes.

Topper, M. B. R., Nava, V., Collin, A. J., Bould, D., Ferri, F., Olson, S. S., Dallman, A. R., Roberts, J. D., Ruiz-Minguela, P., & Jeffrey, H. F., 2019. Reducing variability in the cost of energy of ocean energy arrays. *Renewable and Sustainable Energy Reviews*, *112*, 263-279. https://doi.org/10.1016/ J.RSER.2019.05.032

Von Jouanne, A., & Brekken, T. K. A., 2017. Ocean and Geothermal Energy Systems. *Proceedings of the IEEE*, 105(11): 2147-2165. https://doi.org/10.1109 JPROC.2017.2699558

Wang, L., Ma, X., Kong, H., Jin, R., & Zheng, H., 2022. Investigation of a low-pressure flash evaporation desalination system powered by ocean thermal energy. *Applied Thermal Engineering*, *212*, 118523. https://doi.org/ 10.1016/ J.APPLTHERMALENG.2022.118523

Zhang, H. H., Li, M. J., Feng, Y. Q., Xi, H., & Hung, T. C., 2021. Assessment and working fluid comparison of steam Rankine cycle -Organic Rankine cycle combined system for severe cold territories. *Case Studies in Thermal Engineering*, *28*, 101601. https://doi.org/ 10.1016/J.CSITE.2021.101601